Nuclear Instruments and Methods in Physics Research A 719 (2013) 17–28

Contents lists available at SciVerse ScienceDirect

Nuclear Instruments and Methods in Physics Research A

journal homepage: www.elsevier.com/locate/nima

Beam dynamics performances and applications of a low-energy electron-beam magnetic bunch compressor

C.R. Prokop [a,*], P. Piot [a,b], B.E. Carlsten [c], M. Church [d]

[a] Northern Illinois Center for Accelerator & Detector Development and Department of Physics, Northern Illinois University, DeKalb, IL 60115, USA
[b] Accelerator Physics Center, Fermi National Accelerator Laboratory, Batavia, IL 60510, USA
[c] Acceleration Operations and Technology Division, Los Alamos National Laboratory, Los Alamos, NM 87545, USA
[d] Accelerator Division, Fermi National Accelerator Laboratory, Batavia, IL 60510, USA

ARTICLE INFO

Article history:
Received 5 February 2013
Received in revised form
27 March 2013
Accepted 31 March 2013
Available online 8 April 2013

Keywords:
Photoinjector
Linear accelerator
Electron beam
Magnetic bunch compressor
Space charge
Coherent synchrotron radiation

ABSTRACT

Many front-end applications of electron linear accelerators rely on the production of temporally compressed bunches. The shortening of electron bunches is often realized with magnetic bunch compressors located in high-energy sections of accelerators. Magnetic compression is subject to collective effects including space charge and self interaction via coherent synchrotron radiation. In this paper we explore the application of magnetic compression to low-energy (~40 MeV), high-charge (nC) electron bunches with low normalized transverse emittances (< 5 μm).

1. Introduction

Most of the photoinjectors being used for generation of bright electron bunches for, e.g., free-electron laser (FEL) applications consist of generating and rapidly accelerating the electron bunch to high energy and subsequently shortening the bunch using a magnetic bunch compressor [1]. The only deviation to such a design is the combined acceleration and compression using velocity bunching [2]. Attempts to operate low-energy magnetic bunch compressors have to date been inconclusive [3] or deemed incompatible with the production of low-emittance beams [4]. However, compressing at low energy can be beneficial to mitigate the microbunch instability [5] and is sometimes a necessity, e.g., in compact accelerator-based light sources [6] or injectors for advanced acceleration concepts [7]. In this paper we explore and demonstrate via numerical simulations that low-energy bunch compression performed on a ~40−MeV electron beam can be viable depending on requirements. We especially present trade-off curves between transverse emittance and peak current for several cases of electron-bunch charge. In addition, our simulations are performed with several computer programs thereby enabling a benchmarking of very different approaches for modeling collective effects and especially coherent synchrotron radiation (CSR) [8,9]. Our study considers the magnetic bunch compression planned in the 40–50 MeV photoinjector of the Advanced Superconducting Test Accelerator (ASTA) currently under construction at Fermilab [10,11].

2. Accelerator beamline overview

The compression of a ~40−MeV electron bunch via magnetic compression is investigated for the case of the ASTA photoinjector diagrammed in Fig. 1. The beamline includes a photoemission electron source consisting of a cesium telluride (Cs_2Te) photocathode located on the back plate of a 1+1/2 cell radiofrequency (RF) cavity operating at 1.3 GHz [12]. The cathode is illuminated with a 3-ps ultraviolet laser pulse with uniform radial distribution and a Gaussian temporal profile. The optimum laser rms spot size for minimal emittance depends on the bunch charge and ranges from 80 μm (for 20 pC) to 1.3 mm (for 3.2 nC). The RF gun is surrounded by two solenoidal lenses that control the beam's transverse size and emittance. Downstream of the RF gun, the typical beam energy is ~5 MeV. The bunches are further accelerated up to 50 MeV by two 1.3-GHz superconducting RF (SCRF) accelerating cavities (labeled as CAV1 and CAV2 in Fig. 1). A third SCRF cavity (CAV39) operating at 3.9 GHz will eventually be incorporated to correct for nonlinear longitudinal phase space distortions [13–15]. Because of its superconducting nature, the ASTA facility produces electron bunches repeated at 3 MHz arranged in a 1-ms 5-Hz RF macropulse. The downstream beamline includes

* Corresponding author. Tel.: +1 708 997 1201.
E-mail addresses: cprokop@gmail.com, z171730@students.niu.edu (C.R. Prokop).

0168-9002/$ - see front matter
http://dx.doi.org/10.1016/j.nima.2013.03.068

quadrupoles, steering dipole magnets, and diagnostics stations. A skew-quadrupole channel can be set up as a round-to-flat-beam transformer (RFBT) to convert an incoming angular-momentum-dominated beam into a flat beam with high transverse emittance ratio [16,17]. The beamline also incorporates a four-bend magnetic bunch compressor (BC1) which, consists of four 0.2-m rectangular dipoles (B1, B2, B3, B4) with respective bending angles of $(+,-,-,+)$ 18°. The longitudinal dispersion of BC1 is $R_{56}=-0.19$ m. Finally a single-shot longitudinal phase space diagnostics combining a transverse-deflecting cavity (TDC) with a vertical spectrometer will be installed [18].

The beam dynamics through CAV2 were simulated with ASTRA and optimized using a genetic optimizer for several cases of charge and photocathode drive-laser configurations; see Ref. [19]. The resulting phase space distributions are used as a starting point for transport and compression through the beamline downstream of CAV39. The quadrupoles settings were optimized for the various operating charges using the single-particle dynamics program ELEGANT [20]. The evolution of the nominal betatron functions downstream of CAV39 up to the cryomodule entrance is plotted in Fig. 2.

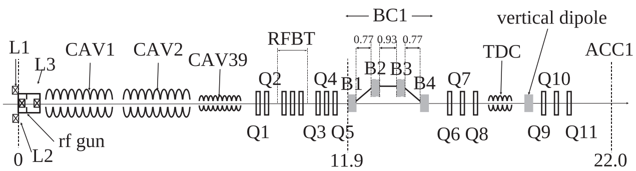

Fig. 1. Injector configuration at ASTA. The "RF gun", "L1" and "L2" respectively correspond to the gun cavity and surrounding solenoid magnets, "CAV1", "CAV2", and "CAV39" are superconducting RF cavities, "RFBT" is the round-to-flat beam transformer, and "BC1" refers to the magnetic bunch compressor, and B1-4 are the dipoles of the chicane, with distance between the dipoles marked in the figure. The number below the beamline indicates the axial positions in meters w.r.t. the photocathode surface.

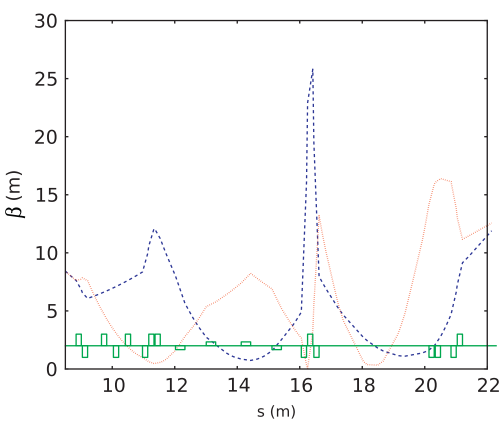

Fig. 2. Evolution of the horizontal (dashed line) and vertical (dotted line) betatron functions through the ASTA injector. The lower line and rectangles indicate the location of quadrupole and dipole (smaller rectangles) magnets. The BC1 compressor is located at $s\in[11.9,15.1]$ m. The origin of the horizontal axis ($s=0$ m, not shown) corresponds to the photocathode surface. (For interpretation of the references to color in this figure caption, the reader is referred to the web version of this paper.)

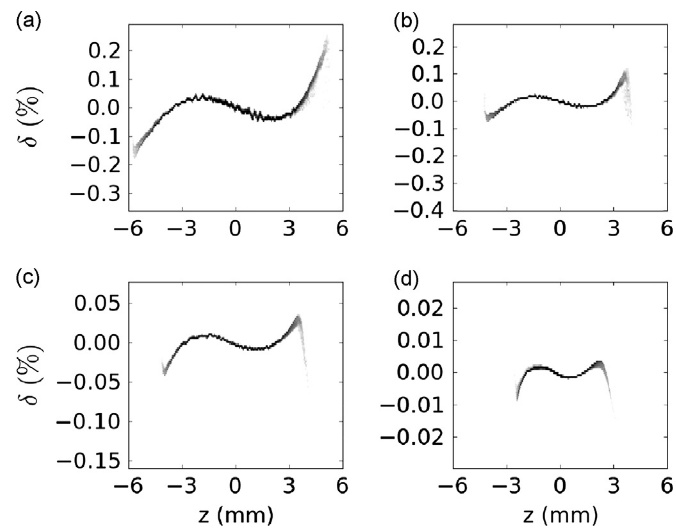

Fig. 3. LPS distributions 0.1-m upstream of dipole magnet B1's entrance face for 3.2 (a), 1.0 (b), 0.25 (c) and 0.02 nC (d) bunches. The distributions were obtained from simulations of the photoinjector beam dynamics in ASTRA; see Ref. [19]. The ordinates $z>0$ correspond to the head of the bunch.

Table 1
Transverse and longitudinal beam parameters 0.1-m upstream of B1 dipole entrance face. Only the Courant–Snyder parameters were fixed while the other parameters depend on the bunch charge or upstream beamline settings.

Parameter	Value	Units
$\beta_{x,i}$	8	m
$\alpha_{x,i}$	3	–
$\beta_{y,i}$	1.6	m
$\alpha_{y,i}$	–1.6	–
$\mathcal{C}$	[1.0,6.0]	m^{-1}
Total energy	38.6	MeV

Table 2
Initial normalized transverse $\varepsilon_{x/y,i}$ and longitudinal $\varepsilon_{z,i}$ emittances and RMS bunch length $\sigma_{z,i}$ for the four cases of charge considered in this paper. The parameters are computed 0.1-m upstream of dipole magnet B1's entrance face.

Q (nC)	$\varepsilon_{x,i}$ (μm)	$\varepsilon_{y,i}$ (μm)	$\varepsilon_{z,i}$ (μm)	$\sigma_{z,i}$ (mm)
3.2	4.43	4.58	82.19	2.56
1.0	2.20	2.22	33.41	1.95
0.250	0.580	0.576	14.37	1.93
0.020	0.296	0.297	2.54	1.26

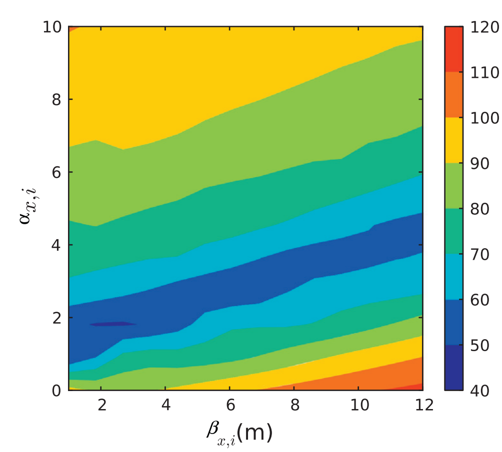

Fig. 4. Contour plot of the final normalized horizontal emittance (ε_x in μm) as a function of the C–S parameters $\beta_{x,i}$ and $\alpha_{x,i}$ 0.1-m upstream of dipole B1. The simulations were performed with CSRTRACK's 1D-Projected model with a bunch charge of 3.2 nC and initial energy chirp of $\mathcal{C}=5.2$ m^{-1}. From this data, we selected the values for our simulations, $(\beta_{x,i},\alpha_{x,i})=(8.0\text{ m},3.0)$. (For interpretation of the references to color in this figure caption, the reader is referred to the web version of this paper.)